

Diblock Copoly(oxyethylene/oxybutylene) $E_{41}B_8$ in Water: Liquid-Crystal Mesophases Studied by Small-Angle X-ray Scattering

J. Patrick A. Fairclough* and Anthony J. Ryan

Department of Chemistry, University of Sheffield,
Sheffield, S3 7HF, U.K.

Ian W. Hamley

Department of Chemistry, University of Leeds,
Leeds, LS2 9JT, U.K.

Hong Li, Ga-Er Yu, and Colin Booth

Manchester Polymer Centre, Department of Chemistry,
University of Manchester, Manchester, M13 9PL, U.K.

Received November 17, 1998

Revised Manuscript Received November 20, 1998

Introduction

Diblock copolymers of ethylene oxide and 1,2-butylene oxide self-associate in aqueous solution. We denote these copolymers E_mB_n , where E = oxyethylene unit [OCH_2CH_2] and B = oxybutylene unit [$\text{OCH}_2\text{CH}(\text{C}_2\text{H}_5)$]. This report concerns copolymer $E_{41}B_8$, which has been studied previously in aqueous solution across a range of concentration,^{1,2} but not by X-ray scattering techniques to reveal the mesophase morphology. Spherical micelles were found to form in dilute solution: e.g., critical micelle concentration, $\text{cmc} \approx 0.2 \text{ g dm}^{-3}$ at 35°C , at which temperature the micellar association number N_w was 30.¹ Considering $T = 35^\circ\text{C}$, as the concentration was increased, the solution first became a soft gel at 18 wt % copolymer and then an isotropic hard gel at 25 wt % copolymer. Alternatively, heating a solution from the mobile low-temperature sol through the soft and hard gels to the high-temperature mobile sol (see Figure 1, adapted from ref 1) could access these phases. These observations were made using three techniques: tube inversion, differential scanning calorimetry, and rheology, with good agreement between them. The notation "soft" and "hard" follows that of Hvidt et al.,³ hard gel denoting an immobile phase (high yield stress), and soft gel a mobile phase with low but significant yield stress, with storage modulus (G') higher than loss modulus (G'').^{1,3} In contrast, the low- T and high- T sol phases (micellar phases) have zero yield stress and $G' < G''$. At concentrations significantly higher than 50 wt %, the gel was seen to be birefringent by polarized light microscopy, the birefringence texture being consistent with a hexagonal structure. It was inferred, but not proven, that the isotropic hard gel was a cubic phase of packed spherical micelles.

Aqueous micellar gels of other diblock E_mB_n copolymers have been studied by small-angle X-ray and neutron scattering, in particular by combined scattering and rheology shear in order to better define the liquid-crystal structures of the gels via scattering patterns from oriented samples.^{4–7} Those studies were of copolymers dissolved in aqueous salt solution (0.2 M K_2SO_4). This was in order to reduce the temperature of gel formation and also to reveal high-temperature features (clouding, high- T gel) which were not accessible in water below 100°C . Cubic (body-centered and face-

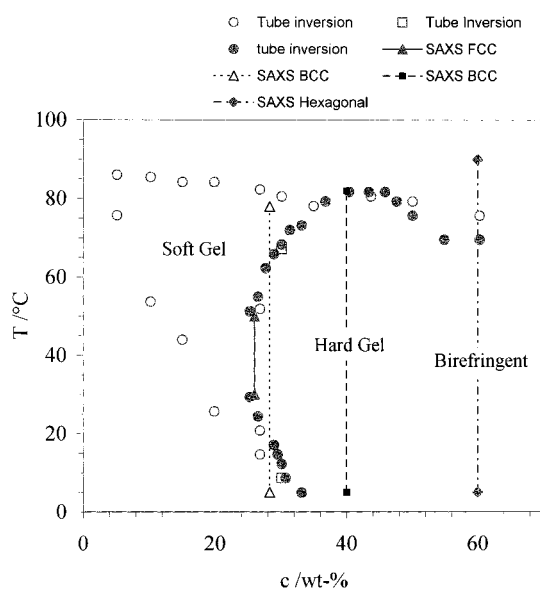


Figure 1. Phase diagram (temperature vs weight fraction of copolymer) for aqueous solutions of copolymer $E_{41}B_8$ showing the soft and hard gel regions, the latter having isotropic and birefringent parts. The diagram is adapted from Figure 2 of ref 1. The temperature range for the ordered phase as determined by SAXS, is marked by symbols on the line. If no symbol is shown the phase exists below 5°C , the start temperature of the slow ramp.

centered) and hexagonal structures were identified. The scattering data presented in this report are for aqueous gels under quiescent conditions. The experiment was designed to probe the gel structure near to the transition from hard to soft gel, as well as to confirm the assignment of the high concentration gel to hexagonal gel (see Figure 1 for details).

Experimental Section

The preparation of copolymer $E_{41}B_8$ has been described elsewhere,² together with the following molecular characteristics: number-average molar mass $M_n = 2400 \text{ g mol}^{-1}$ and 76 wt % E from ^{13}C NMR spectroscopy; molar mass ratio $M_w/M_n = 1.04$ from gel permeation chromatography.

Gels of concentration 26, 28.5, 40, and 60 wt % (as indicated in Figure 1) were prepared by weighing water and copolymer into closed tubes, heating the tubes to 90°C (fluid state) for 2 h, and then storing them at 10°C for 1 day or more. For X-ray scattering, the gels were drawn as rapidly as possible into thin glass capillaries, which were then sealed. Small-angle X-ray scattering (SAXS) experiments were performed on beamline 8.2 of the SRS at the CCLRC Daresbury Laboratory, Warrington, U.K., details of which have been given elsewhere.⁸ The capillaries were heated in a Linkam capillary hotstage from 5 to 90°C and then back to 5°C at $1\text{--}2^\circ\text{C min}^{-1}$. The scattering from the solutions was collected by a multiwire area detector for the viscous samples and a quadrant linear detector for the low viscosity materials. The data from both detectors were corrected for background scattering from the camera and capillary sample holder with a flat field correction applied to compensate for detector nonlinearity. The choice of detector is important as the high viscosity samples are oriented during loading; only the area detector would detect this. If scattering from such a sample were collected on a linear detector, the points of high scattering intensity might fall outside the window of detection, leading to incorrect intensities during the integration across the detector. Vertical slices were taken from

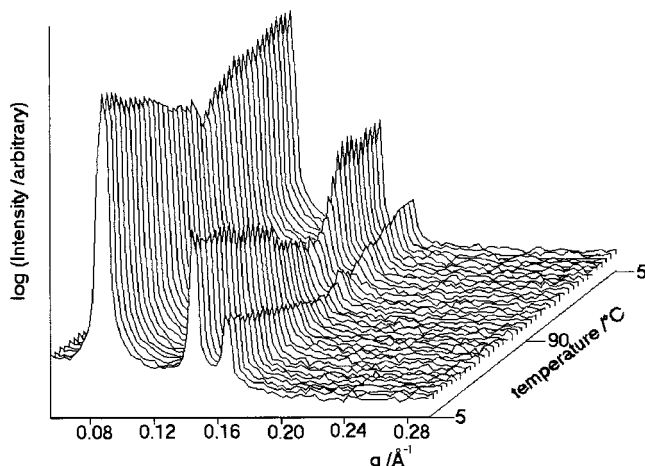


Figure 2. Scattering intensity vs q vs temperature for 60 wt % $E_{41}B_8$ in water. Note the persistence of the hexagonal ordering into the soft gel phase.

the area data for the oriented. For unoriented samples, a radial integration was applied to obtain better precision for the weakly scattering disordered sol systems.

Results and Discussion

SAXS patterns, obtained as a function of temperature for the 60 wt % solution of the copolymer, are shown in Figure 2. The plot is of $\log(\text{intensity})$ vs $q = (4\pi/\lambda) \sin(\theta/2)$ vs temperature, where λ is the wavelength of the incident radiation (1.54 Å) and θ is the scattering angle.

The pattern in Figure 2 shows orders of reflection at $q/q^* = 1, \sqrt{3}$, and $\sqrt{4}$, where q^* is the q value of the first-order reflection, which is consistent with a structure composed of hexagonally packed cylindrical micelles. The periodicity ranges from 70.6 to 72.2 Å over a temperature range 5–90 °C. As can be seen in Figure 2, the intensity of scattering is reduced at temperatures above 70 °C, which is the high-temperature limit of immobile hard gel as detected by tube inversion and rheology.¹ However, the hexagonal structure clearly persists in the mobile phase in the range $T = 70$ –90 °C.

For 40 wt %, the scattering pattern (not shown) shows strong reflections with q/q^* ratios of $1:\sqrt{2}:\sqrt{3}$, which is characteristic of a bcc structure, presumed to consist of close-packed spheres. The spacings indicate a periodicity of 84 Å. This is consistent with the previous rheology¹ results indicating a hard gel with a modulus G' of 10^5 Pa.¹ The system is disordered in the temperature range 85–90 °C.

Scattering patterns from the 28.5 wt % gel (not shown), obtained in the temperature range 20–70 °C, show weak reflections at q/q^* ratios of $1:\sqrt{2}:\sqrt{3}$, consistent with a underlying bcc structure that disorders to the sol phase at 79 °C.

The structure of the other dilute gel (26 wt %) was investigated in more detail. When heated from 5 °C, the system samples the soft and hard gel regions, with transition temperatures as follows: 18 °C (sol → soft gel), 26 °C (soft → hard gel), 55 °C (hard → soft gel) and 82 °C (soft-gel → sol).

The scattering pattern in Figure 3 provides limited evidence of structure in the temperature range of the hard gel, but none outside that region. We can tentatively assign this structure as fcc structure, this being based on q/q^* ratios of $1:\sqrt{4/3}$ with a periodicity of 50

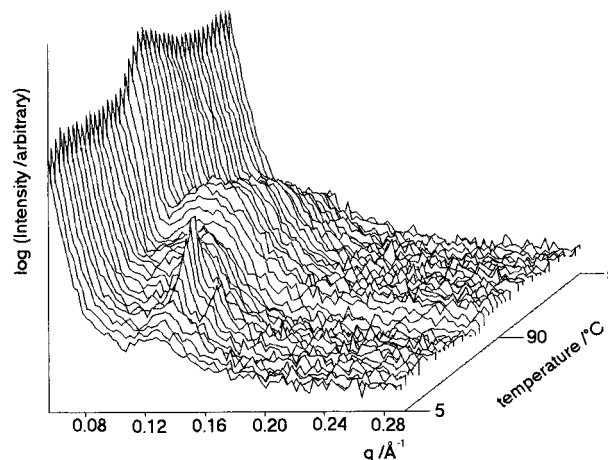


Figure 3. Scattering intensity vs q vs temperature for 26 wt % $E_{41}B_8$ in water.

Å. From the scattering patterns the transition temperature from soft to hard gel occurs at 30 °C, reverting back to soft gel at 45 °C. Overall, it is interesting to note that the transition temperatures measured by scattering do not correspond exactly to those measured by rheology (tube inversion and rheology). For the hexagonal and bcc gels (60 and 40 wt %), structure is detected at temperatures above the hard gel limit. A similar result has been reported previously for an $E_{40}B_{10}$ micellar gel in 0.2M K_2SO_4 .⁴ The effect may be due to the formation of highly defective phases, thus conferring mobility in the system and determining the overall rheological response.

As discussed by Pople et al.,⁴ the defects allow domains of ordered phase to slip over each other. SAXS is sensitive to the amount of ordered material present, i.e., the number of grains, and insensitive to the defects; rheology is sensitive to the defects. As the transition temperature is approached, defects and domain boundaries play an increasing role in determining the rheological response. For the fcc gel (26 wt %) this was not the case, as the transitions defined by SAXS fell within those measured by rheology. However, the concentration dependence of the transition temperature is extremely large in the concentration range 24–28 wt % (see Figure 1), and the difference may well arise from a small uncertainty in concentration. It is interesting to compare that system with $E_{41}B_8$. In both systems a low concentration fcc phase exists this transforms to bcc with increasing concentration, however the transition $\text{fcc} \rightarrow \text{bcc}$ can be thermally induced in the $E_{40}B_{10}$ system^{4,5,9} unlike the present $E_{41}B_8$ system.

Acknowledgment. The authors thank Dr B.U. Komanschek for his assistance during the experiments at the CCLRC SRS Daresbury Laboratory. Financial assistance was provided by the EPSRC (U.K.).

References and Notes

- Li, H.; Yu, G.-E.; Price, C.; Booth, C.; Hecht, E.; Hoffmann, H. *Macromolecules* **1997**, *30*, 1347.
- Yu, G.-E.; Yang, Z.; Ameri, M.; Attwood, D.; Collett, J. H.; Price, C.; Booth, C. *J. Phys. Chem., B* **1997**, *101*, 4394.
- (a) Hvdt, S.; Jorgensen, E. B.; Brown, W.; Schillen, K. *J. Phys. Chem.* **1994**, *98*, 12320. (b) Almgren, M.; Brown, W.; Hvdt, S. *Colloid Polym. Sci.* **1995**, *273*, 2.
- Pople, J. A.; Hamley, I. W.; Fairclough, J. P. A.; Ryan, A. J.; Komanschek, B. U.; Gleeson, A. J.; Yu, G.-E.; Booth, C. *Macromolecules* **1997**, *30*, 5721.

- (5) Hamley, I. W.; Pople, J. A.; Fairclough, J. P. A.; Terrill, N. J.; Ryan, A. J.; Booth, C.; Yu, G.-E.; Diat, O.; Almdal, K.; Mortensen, K.; Vigild, M. *J. Chem. Phys.* **1998**, *108*, 6929.
- (6) Hamley, I. W.; Pople, J. A.; Booth, C.; Yang, Y.-W.; King, S. M. *Langmuir* **1998**, *14*, 3182.
- (7) Hamley, I. W.; Pople, J. A.; Fairclough, J. P. A.; Ryan, A. J.; Booth, C.; Yang, Y.-W. *Macromolecules* **1998**, *31*, 3906.
- (8) Bras, W.; Derbyshire, G. E.; Clarke, S.; Devine, A.; Komanschek, B. U.; Cooke, J.; Ryan, A. J. *J. Appl. Crystallogr.* **1994**, *28*, 26.
- (9) Hamley, I. W.; Pople, J. A.; Diat, O. *Colloid Polym. Sci.* **1998**, *276*, 446.

MA981775J